Valve seat angle influence on losses in valves for steam turbines

Vaclav Slama[1,2*], *David* Simurda[3], *Petr* Kollross[1]

[1]Doosan Skoda Power, Tylova 1/57, 301 28 Pilsen, Czech Republic
[2]University of West Bohemia, Power System Engineering Department, Univerzitni 8, 306 14 Pilsen, Czech Republic
[3]Institute of Thermomechanics of the Czech Academy of Sciences, Dolejskova 1402/5, 182 00 Praha, Czech Republic

Abstract. Losses in valve assemblies have a significant influence on turbines´ efficiency. Therefore, performing pressure loss analysis to enhance the valve design has always been one of the traditional issues. Valves can differ in many ways in terms of their design. This paper aims to show the influence of the valve seat angle, which is one of the characteristic design dimensions. In order to achieve this, different results from a wide range of measurements on two different models are used. Regarding the first model with a 60° valve seat angle, the measurement was performed in the Aerodynamic laboratory of the Institute of Thermomechanics of the Czech Academy of Sciences. The measurement of the second model with a 90° valve seat angle was performed in the Doosan Skoda Power experimental lab. Differences are described in the form of a total loss coefficient and a flow contraction coefficient. The results are complemented by flow fields from numerical simulations performed on both valve models using a package of ANSYS software tools.

1 Introduction

Different valve designs exist based on complex requirements such as safe operation, a reasonable price, low pressure losses, and a steam turbine governing method [1]. Some typical as well as extraordinary ones are shown in [2]. Each design part of the valve somehow influences the losses in the valve. This influence can be significant or negligible. This paper describes the influence of the valve seat angle in two particular valve designs.

Doosan Skoda Power has performed many studies connected with valves for steam turbines, for example [3-7]. These papers show and analyze different valve models for measurements and numerical simulations using numerical and measured data. There were evaluated pressure losses as well as unsteady pressure fluctuations. A detailed analysis from the theoretical point of view is also going to be presented in [8]. However, the direct comparison of pressure losses caused by different valve seat angles has yet to be shown.

The schematic picture with valve seat angle α is shown in Fig. 1. In practice, there are often used two most typical valve seat angles: 60° and 90°. The valve models on which

* Corresponding author: vaclav.slama@doosan.com

measurements were performed are shown in Figs. 2 and 3, respectively. On the left, there is a valve assembly with a trough-flow valve chamber where each control valve seat angle is 60°. For the study presented in this paper, the results regarding the second valve in the chamber (valve B) are used only (valve A was always closed). On the right, there is a valve where the seat angle is 90°. In this case, there was only one valve.

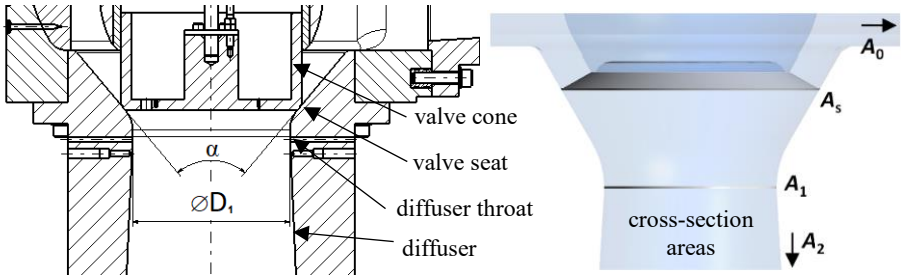

Fig. 1. Schematic picture of the valve seat angle and other characteristic valve features.

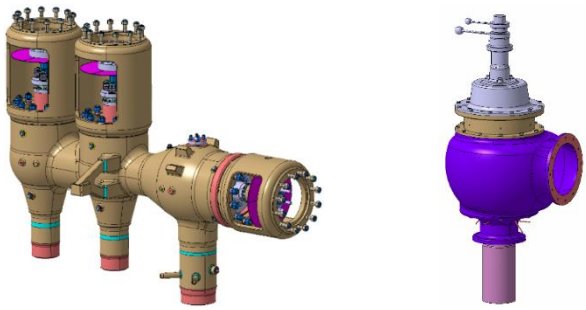

Fig. 2. Assembly of control valves, the valve seat angle of 60° (left) and 90° (right).

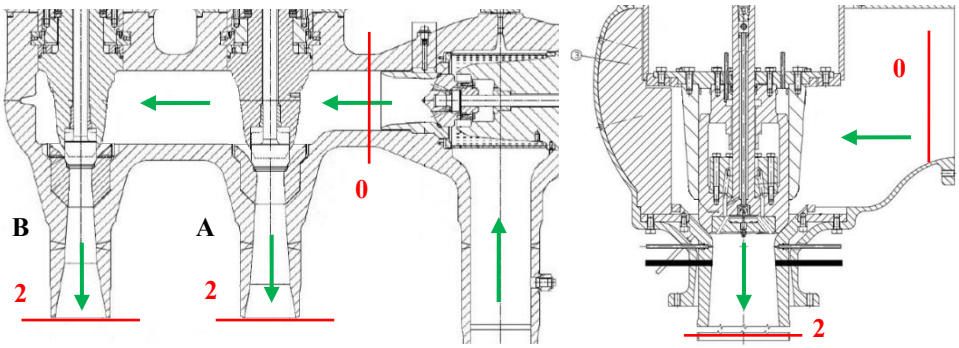

Fig. 3. Cross-section through the assembly of control valves, 60° (left) and 90° (right).

The typical way to describe a relationship between the mass flow ratio q, the pressure ratio ε_2, and the flow-through area, which depends on the valve cone lift z, is to use the so-called flow characteristics. An example of a typical valve flow characteristic is in Fig. 4, where three theoretical curves are depicted. Each of them corresponds to one relative valve cone lift $\bar{z} = z/D_1$. Mass flow ratio $q = m/m_*$, where m_* is the critical mass flow depending on the flowing medium inlet parameters and the cross-section area of the diffuser throat A_1. The pressure ratio $\varepsilon_2 = p_2/p_{0t}$ indicates the ratio of the static pressure at the valve outlet and the total pressure at the valve inlet. In this paper, subscript 0 means the valve inlet, 1 means the diffuser throat and 2 means the valve outlet. The dashed line presents the usual operating range for a typical steam turbine. With decreasing ε_2, the choked flow appears which means

that q cannot grow anymore. For each relative valve cone lift $\bar{z}$, it appears when reaching ratio ε_{*z}. The shown curve from all ε_{*z} is purely illustrative here. The maximum mass flow ratio for each valve cone lift is q_{*z}.

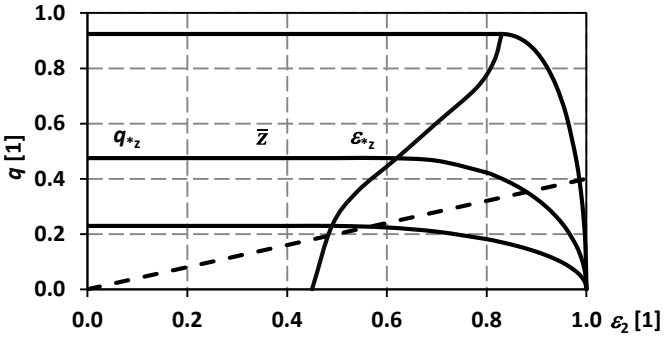

Fig. 4. Example of a valve flow characteristic.

2 Experimental and numerical models

The experimental model of the valve assembly with the valve seat angle of 60° is shown in Fig. 5 on the left. It was installed in the Aerodynamic laboratory of the Institute of Thermomechanics of the Czech Academy of Sciences, where a wide range of measurements was performed. Measurement positions 0 and 2 are shown in Fig. 3, where four static pressure taps evenly distributed around a pipe circumference were installed. In addition, the total pressure at the inlet of the valve chamber was measured by a Prandtl probe. The mass flow rate was measured in each outlet pipeline by using the Annubar Deltatop DP 62D probe and Thermometers Pt100. Other details about measurements are presented in [3, 4]. The model of the valve assembly with the valve seat angle of 60° is shown in Fig. 5 on the right. It was installed in the experimental hall in Doosan Skoda Power. The measurement was similar to the above-mentioned one [9]. The measured positions are also shown in Fig. 3.

Fig. 5. Valve assembly models installed in wind tunnels, 60° (left) and 90° (right).

The models for numerical simulations, see Fig. 6, were created in accordance with the experimental ones. The mesh was created in ANSYS ICEM 2021R1, with a hexahedral mesh for pipelines and a tetrahedral mesh for valves. An appropriate boundary layer ensuring that the maximum value of $y+$ is lower than 5 was created on all walls. ANSYS CFX 2019R1

was used as a solver. It provided the steady state solution with a turbulence model k-ω SST. A high-resolution scheme was used to deal with the advection term and the turbulence modeling. The medium was considered dry air according to the measurement. Inlet boundary conditions (a total pressure and a static temperature) were specified according to the measured results. Outlet static pressures were defined according to the required ε_2. More details about numerical simulations on the assembly with the valve seat angle of 60° are described in [3, 4]. The case of 90° is similar. The required data were evaluated in planes upstream and downstream of the valve (see positions 0 and 2 in Fig. 3) using a mass-flow average abs method.

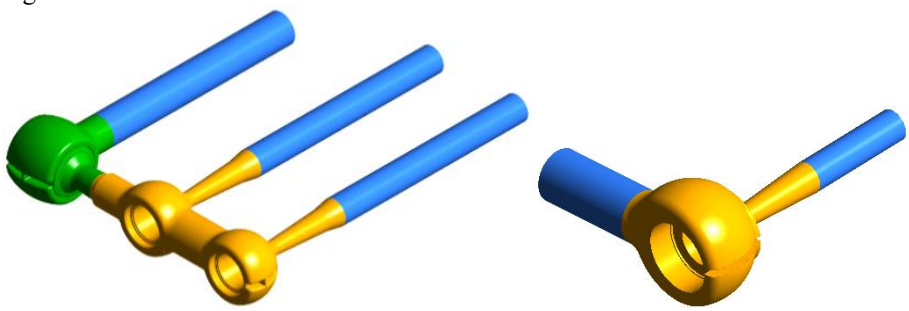

Fig. 6. Numerical models of valves, 60° (left) and 90° (right).

3 Results and discussion

At first, valve flow characteristics for both cases were created based on measured data. Results are in Fig. 7. The greater the q for the same ε_2, the lower the pressure loss. It also means the greater the ε_2 for the same q, the lower the pressure loss.

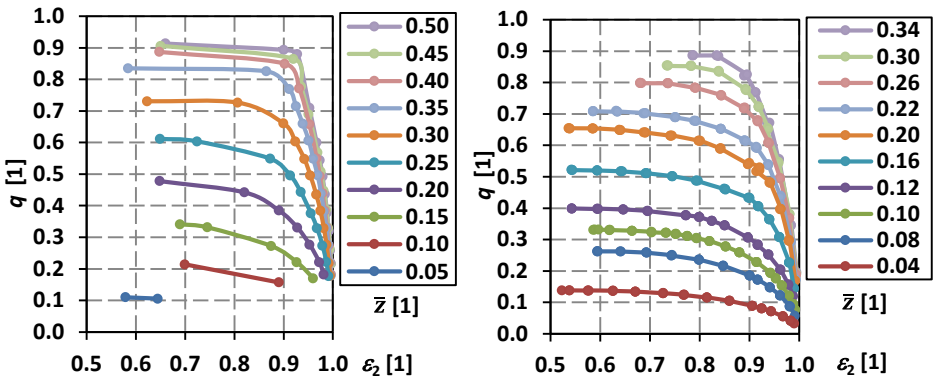

Fig. 7. Valve flow characteristics, the valve seat angle of 60° (left) and 90° (right).

Second, the numerical results, which are further used to analyze internal flow fields, were compared with the experimental ones in the form of the flow characteristics as well. It is shown in Fig. 8 and 9, respectively. The black crosses present the numerical results (CFD). It was found that they followed the curves from measured data very well. There are differences, but not greater than ±10 % in terms of the mass flow ratio. It also includes the greatest detected difference shown in Fig. 9. Another important fact is that the measurement was not carried out for lower pressure ratios due to the limited funds (the lower the pressure ratio, the more expensive the measurement). However, it is assumed that the related flow characteristic curves go the same way. Therefore, the differences may be as minor as for the cases with a greater pressure ratio.

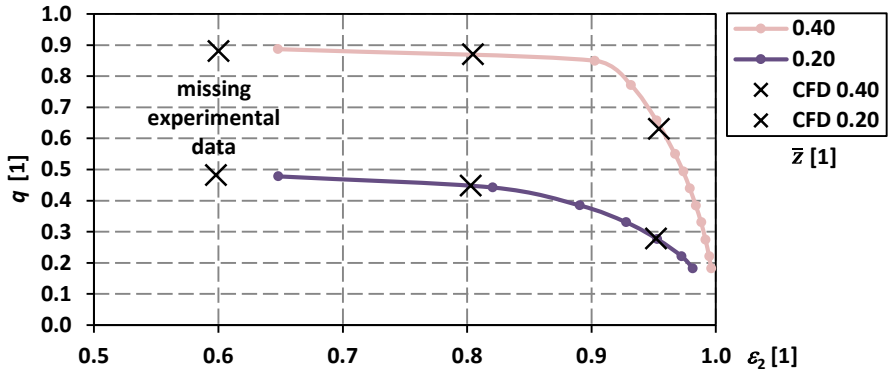

Fig. 8. Valve flow characteristics, the valve seat angle of 60°, comparison between CFD and experimental results.

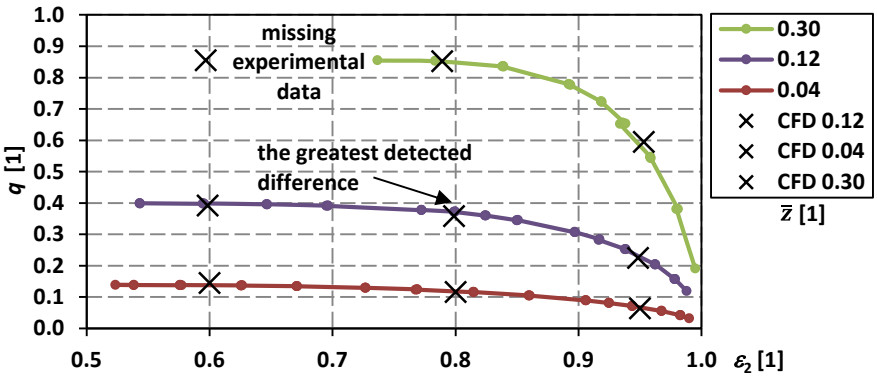

Fig. 9. Valve flow characteristics, the valve seat angle of 90°, comparison between CFD and experimental results.

Going back to the results showed in Fig. 7, the first important thing to be noticed is that measurements were not performed for the same $\bar{z}$. The reason is that the measurements were prepared and performed independently and with no intention to directly compare them. Furthermore, the greater the α, the greater the increase in the mass-flow area, therefore increase in q. It is shown later in Fig. 10. Due to this, the simple comparison of valve characteristics is not possible. However, the results can be compared using the characteristic quantities q_{*z} and ε_{*z}. The second important thing to be noticed is that in the case of 60°, there are not enough measured points for $\bar{z} = 0.05$ and 0.10 to detect the values of q_{*z} and ε_{*z}. Because it would be troublesome to repeat the measurements or add numerical simulations, the curves were extrapolated in order to comply with equation 1 which is introduced later. Due to this, the results for $\bar{z} = 0.05$ and 0.10 in Figs. 10 and 11 are only illustrative and are not considered for discussions. Fortunately, such small lifts are not important when analyzing pressure losses for practical cases where valves are at least more than half open. When extracting q_{*z} and ε_{*z}, their dependencies on $\bar{z}$ can be depicted as in Fig. 10.

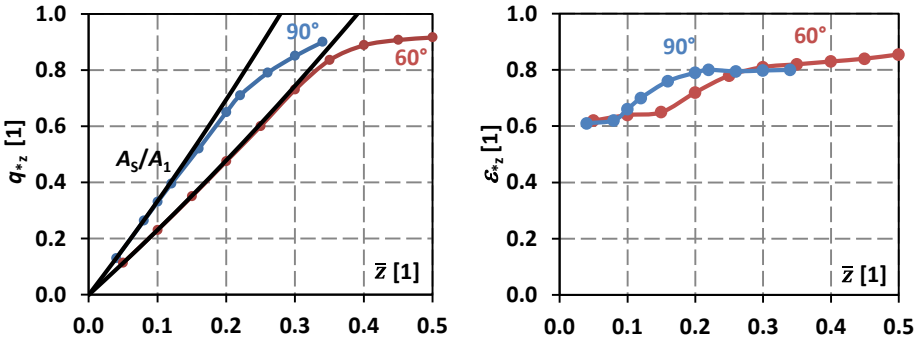

Fig. 10. Critical mass flow ratio (left) and critical pressure ratio (right) dependences on the relative valve cone lift.

In Fig. 10 on the left, the important feature can be seen. In the case of $\alpha = 90°$, there is a faster increase in the cross-section area under the valve cone A_s with increasing $\bar{z}$ than in the case of $\alpha = 60°$. It is shown by the black lines. It is also the reason why in the case of $\alpha = 60°$, the greater $\bar{z}$ can be achieved. It also corresponds to the faster ending of the linear increase in q_{*z}. To achieve the same q_{*z}, the smaller valve cone lift is sufficient for the case of $\alpha = 90°$ than for the case of $\alpha = 60°$. This can be considered an advantage from the design point of view since the valve spindle and chamber can be shorter, therefore cheaper. Nevertheless, the disadvantage is that there are greater pressure losses, as shown further in Fig. 11.

Comparing the quality of valves using q_{*z} and ε_{*z} is illustrative but not practical because it cannot be used for predicting the pressure loss for greater ε_2. This could be done using equation (1), where the total loss coefficient in the valve ζ_v and the flow contraction coefficient μ_v are introduced. As a result, q can be calculated for each ε_2. This equation is also practical to approximate the curves in valve flow characteristics.

$$q = \left(\frac{\gamma+1}{2}\right)^{\frac{1}{\gamma-1}} \sqrt{\frac{\gamma+1}{\gamma-1}} \sqrt{\frac{1-\varepsilon_2^{\frac{\gamma-1}{\gamma}}}{\zeta_v}} \left(1 - \frac{1-\varepsilon_2^{\frac{\gamma-1}{\gamma}}}{\zeta_v}\right)^{\frac{1}{\gamma-1}} \frac{A_s}{A_1}\mu_v \qquad (1)$$

The flow contraction coefficient μ_v presents the fact that the real flow area is always smaller than the theoretical areas A_s and A_1. The actual mass flow is, therefore, lower than the theoretical one. It is caused by the flow detachment and the backflow that occurs under the valve cone. Due to this, the velocity in the diffuser throat and under the valve cone is always uneven. It is significantly greater near the diffuser walls and lower in the middle. Other effects, such as friction, are supposed to be included in ζ_v. γ is the heat capacity ratio, A_s is the cross-section area between the valve seat and the valve cone, and A_1 is the cross-section area in the diffuser throat, see Fig. 1 on the right. Equation (1) can be used assuming that for each relative valve cone lift $\bar{z}$, coefficients μ_v and ζ_v are constant. Then ζ_v can be calculated from ε_{*z}, and μ_v can be calculated from q_{*z}. Both ε_{*z} and q_{*z} can be determined from the results of measurements or numerical simulations for each $\bar{z}$, as it is shown in Fig. 10. γ is defined by the flowing medium, and A_s/A_1 is defined by the valve geometry. Other facts about this amended empirical equation (1), which is based on the source [2], can be found in [5, 6]. The most illustrative description and its derivation is going to be published in [8]. The important is that this approach using coefficients ζ_v and μ_v is valuable for analyzing and comparing different valves.

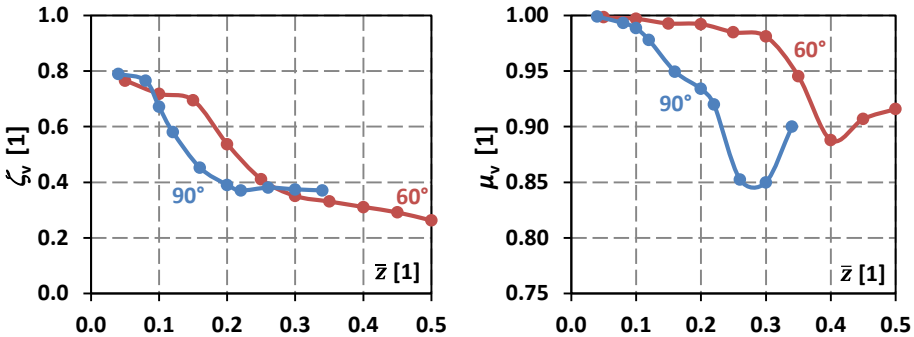

Fig. 11. Total loss coefficient (left) and flow contraction coefficient (right) dependences on the relative valve cone lift.

As mentioned before, values of $\bar{z} \leq 0.10$ are not relevant. For $0.10 < \bar{z} \leq 0.25$, there is a smaller total loss coefficient in the valve ζ_v for the case of $\alpha = 90°$, see Fig. 11 on the left. For $\bar{z} \geq 0.25$, ζ_v is lower for the case of $\alpha = 90°$. It means that the pressure losses could be lower for the lower valve cone lifts in the case of $\alpha = 90°$. However, for the greater valve cone lifts, the pressure losses are lower for the case of $\alpha = 60°$. For practical use of valves, we are interested in pressure losses especially for greater valve cone lifts, often for fully open valves only. Therefore, the valve with $\alpha = 60°$ is better. In addition, the flow contraction coefficient μ_v is in all cases lower for the case of $\alpha = 90°$ even in the area of lower ζ_v. The case of $\alpha = 90°$ is, therefore, more susceptible to changes in the flow cross-section area. To some extent, it can lead to undesirable pressure fluctuations which are described in [10]. Fortunately, such phenomena were not observed during typical operating conditions, as it is reported in detail in [7].

There are two reasons for greater losses for the fully open valve with $\alpha = 90°$. In the valve with $\alpha = 60°$, there is a smaller influence of the wake under the valve cone and a greater radius between the valve seat and the diffuser throat. Regarding the wake position, in order to achieve the same flow area for the case of $\alpha = 60°$, the valve cone lift has to be greater. Therefore, the wake occurring under the valve cone is further from the diffuser throat area. As a result, it has less influence on the flow. Regarding the greater radius, it is similar to the flow in pipe bends [11, 12], where it can be found that the greater the radius, the lower the pressure loss.

In order to see what happens inside the flow field, numerical simulations were performed. For each case, two typical valve cone lifts were chosen: the almost fully open valve and the half-closed valve. In addition, the almost closed valve was added for the case with $\alpha = 90°$. Three pressure ratios were calculated: $\varepsilon_2 = 0.60$, where the flow should be chocked; $\varepsilon_2 = 0.80$, where the flow can be chocked or local areas with $Ma > 1$ can appear; and $\varepsilon_2 = 0.95$, where the flow is subsonic. Results are shown in Figs. 12-16. In each picture, the sonic line is shown by the black line. This line was depicted as the region of $0.98 \leq Ma \leq 1.02$ because the exact line of $Ma = 1$ was hardly visible. Therefore, the line is sometimes wider than expected.

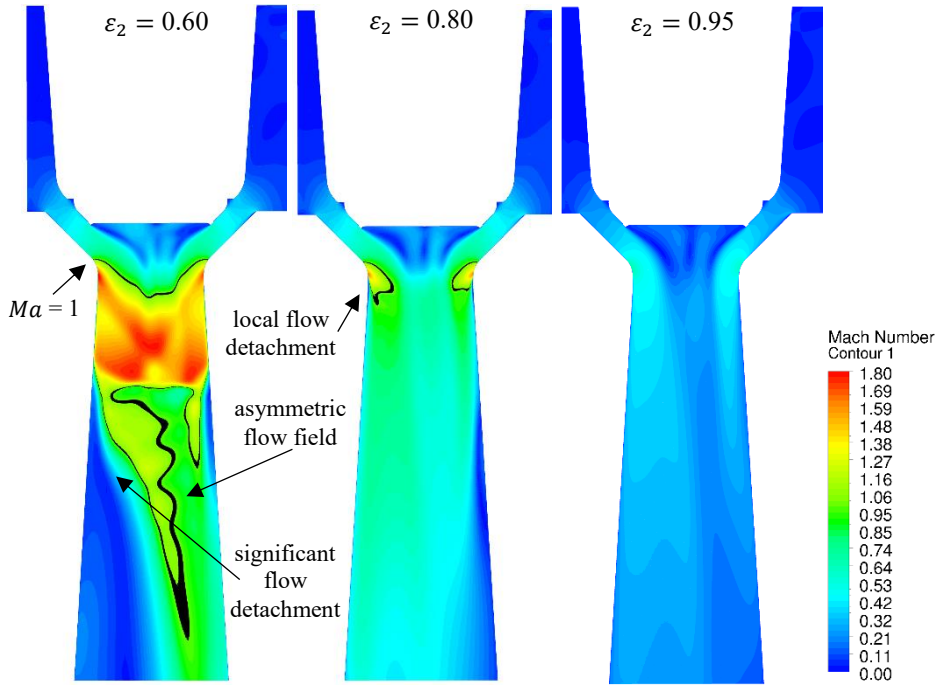

Fig. 12. Mach number, a cross-section through the valve with the seat angle of 90° and the relative valve cone lift of 0.30.

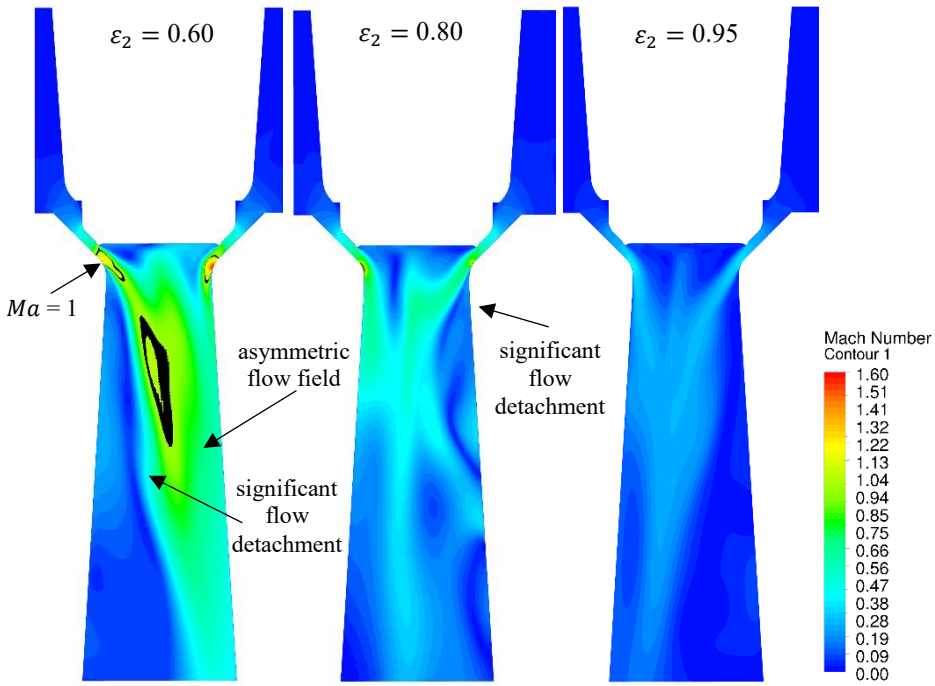

Fig. 13. Mach number, a cross-section through the valve with the seat angle of 90° and the relative valve cone lift of 0.12.

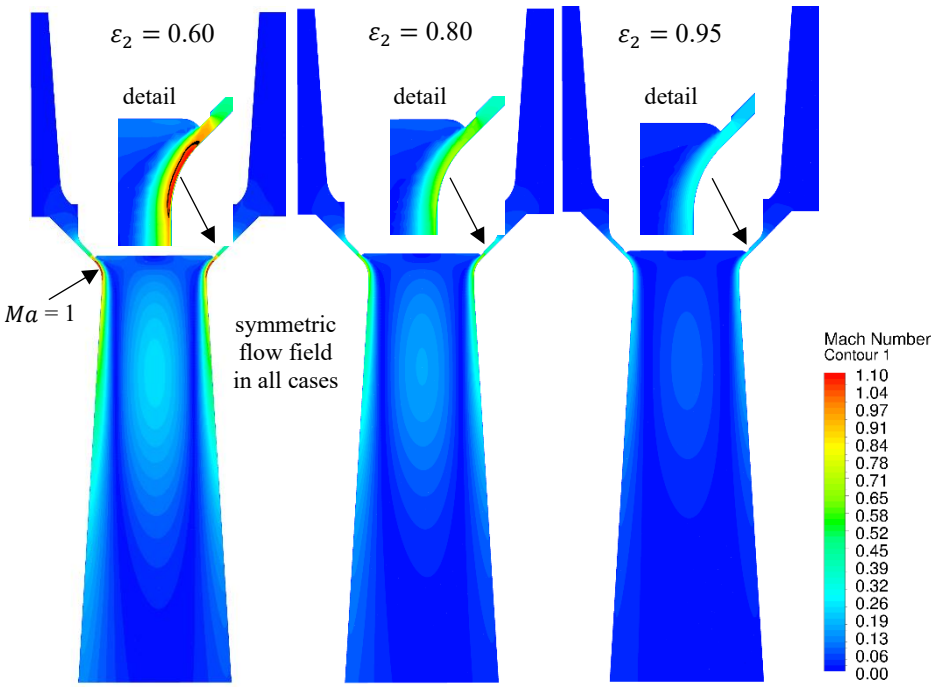

Fig. 14. Mach number, a cross-section through the valve with the seat angle of 90° and the relative valve cone lift of 0.04.

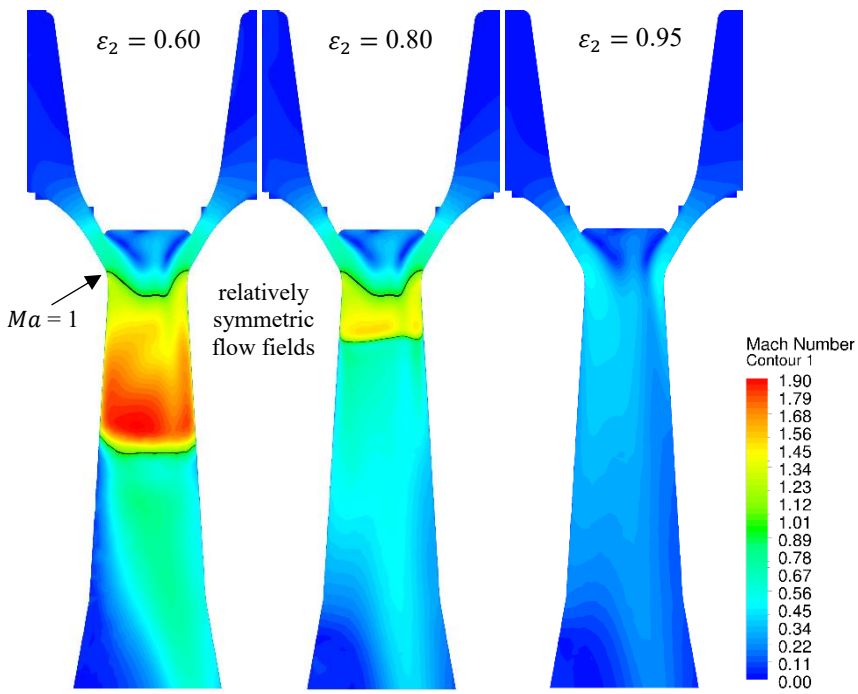

Fig. 15. Mach number, a cross-section through the valve with the seat angle of 60° and the relative valve cone lift of 0.40.

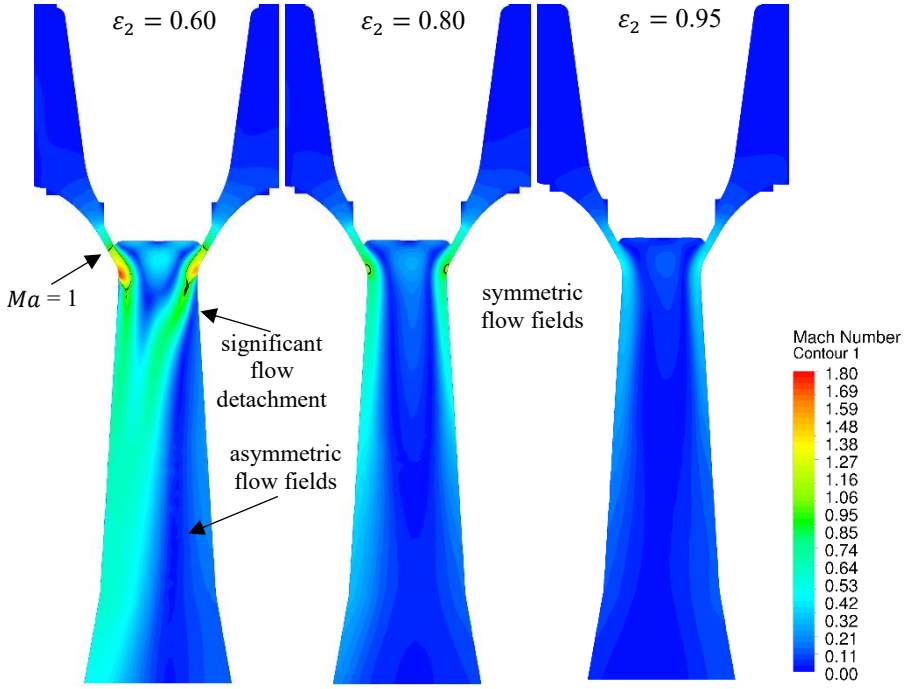

Fig. 16. Mach number, a cross-section through the valve with the seat angle of 60° and the relative valve cone lift of 0.20.

If we compare the cases of almost fully open valves in Figs. 12 and 15, it can be seen that the flow field is significantly asymmetric and with a remarkable flow detachment in the case of $\alpha = 90°$. The lower the ε_2 is, the more significant flow asymmetry can be seen. On the contrary of this, the flow is rather symmetric in the case of $\alpha = 60°$. Another fact worth mentioning is that the sonic line is located in the diffuser throat (area A_1) in Figs. 12 and 15. This is because the area in the diffuser throat is the smallest one. Therefore, it determines the mass flow. The sonic line is not exactly in the diffuser throat, but it is distorted by the influence of the valve cone lift. This is the effect represented by μ_v. When the valve is more closed, as it is in Figs. 13 and 16, the sonic line is under the valve cone (area A_s). It is because this area is the smallest one in such a case. The sonic line is again not exactly in the smallest area, but it is slightly distorted. In addition, the flow field behavior is more complicated. According to the ε_2, the sonic line could be local, as it is shown in Fig. 12 for $\varepsilon_2 = 0.80$ and in Fig. 13 for $\varepsilon_2 = 0.60$. It was not observed in the case of $\alpha = 60°$ as it is in Figs. 15 and 16. The fact that the flow field is more symmetric in the case of $\alpha = 60°$ means that pressure losses should be lower there. It is in accordance with evaluated coefficients μ_v and ζ_v in Fig. 11. When the valve is almost closed, as it is shown in Fig. 14, the flow is fully symmetric and without the flow detachment. The same situation would appear in the case of $\alpha = 60°$.

4 Conclusions

The influence of the valve seat angle was analyzed using available results from the measurement on two different valve models: with $\alpha = 60°$ and 90°. It was shown that a direct comparison using the valve flow characteristics is not possible. Therefore, the comparison was performed using the total loss coefficient in the valve ζ_v and the flow contraction coefficient μ_v.

It is shown that when opening the valve (increasing the relative valve cone lift $\bar{z}$) there is a steeper increase in the case of α = 90° than in case of 60°. This increase is caused by the steeper increase in the mass flow area. According to the results of ζ_v, the pressure losses could be lower for the lower valve cone lifts in the case of α = 90°. However, for the greater valve cone lifts, the pressure losses are lower for the case of α = 60°. According to the results of μ_v, it is in all cases lower for the case of α = 90° even in the area of lower ζ_v. The case of α = 90° is, therefore, more susceptible to changes in the flow cross-section area. The reason why the case of α = 60° is better in terms of losses can be explained by a smaller influence of the wake under the valve cone and a greater radius between the valve seat and the diffuser throat. The results, which are based on the results of measurements on the models, were supported by the flow fields from numerical simulations. For the case of α = 90°, the flow field tends to be very asymmetric and with significant flow detachments than in the case of α = 60°, where the flow field is rather symmetric.

In the future, it would be attractive to simulate and evaluate more flow fields (relative valve cone lifts and boundary conditions) to see and adequately describe phenomena that can appear in the valve. The presented evaluation uses the coefficients μ_v and ζ_v is also going to be used for other valve assemblies.

This research was based on the support of the Technology Agency of the Czech Republic, National Center for Energetics TN02000025.

References

1. J. Becvar et al.: *Thermal turbines* (*Tepelné turbíny*), SNTL, 1968
2. A. E. Zaryankin, B. M. Simonov: *Control and stop-control valves of steam turbines* (*Регулирующие и стопорнорегулирующие клапаны паровых турбин*), Moscow Energetic Institute, Moscow, ISBN 5-7046-1143-5, 2005
3. V. Slama, L. Mrozek, B. Rudas, D. Simurda, J. Hala, M. Luxa: *Experimental and numerical study on pressure losses and flow fluctuations in a high-pressure valve assembly of steam turbine governing system*, ASME Turbo Expo 2020, GT2020-14474, Virtual, Online conference, September 2020
4. V. Slama, B. Rudas, D. Simurda, J. Hala, M. Luxa: *Pressure losses analysis in two high-pressure steam turbine control valves situated in one valve chamber*, ASME Turbo Expo 2022, GT2022-78969, Rotterdam, the Netherlands, June 2022
5. V. Slama, L. Mrozek, L. Tajc, M. Klimko, P. Zitek: *Flow analysis in a steam turbine control valve with through-flow valve chamber*, Journal of Nuclear Engineering and Radiation Science, NERS-20-1141, November 2020
6. L. Mrozek, V. Slama, K. Sedlak, L. Tajc: *Analysis of losses in steam turbine control valves*, AIP Conference Proceedings 2323, 060003 (2021), March 2021
7. V. Slama, D. Simurda, L. Mrozek, L. Tajc, J. Hala, T. Radnic: *Pressure losses and oscillations in a compact valve of a steam turbine*, MATEC Web of Conferences 345, 00027 (2021), October 2021
8. V. Slama, B. Rudas, D. Simurda, J. Hala: *Pressure losses analysis and its prediction in typical valve designs for steam turbines*, ASME Turbo Expo 2023, GT2023-101134, Boston, MA, USA, June 2023
9. P. Kollross, L. Tajc: *An experimental research of the DSPW steam turbine control valve*, AIP Conference Proceedings 2189, 020012, November 2019

10. C. Domnick, D. Brillert: *Flow-induced steam valve vibrations – a literature review of excitation mechanisms, preventive measures, and design improvements*, J. Eng. Gas Turbines Power, 141(5): 051009 (14 pages), GTP-18-1034, May 2019
11. M. E. Dejc: *Technical dynamics of gases* (*Technická dynamika plynů*), SNTL, Praha, 1967
12. I. E. Idelchik: *Handbook of hydraulic resistance 2nd edition*, ISBN 0-89116-284-4, 1975